6. Experimental Procedure

6.1 Introduction

The experimental verification was carried out on a scale model of a mineshaft and conveyance which has been constructed for past research at the University of Pretoria. This tenth scale model had been used to simulate dynamic, scaled down conditions, similar to real-life applications. For the purposes of this study, the existing model was adapted to accommodate the dynamic bending deceleration systems (refer: Figure 5, Figure 30). A piezoelectric accelerometer was attached to the model cage, and acceleration readings were captured during the experiment (refer: Figure 28). The data was recorded by means of a laptop and 'spider' (refer: Figure 29). The 'spider' is a data buffer, implying that it stores data and then transfers it to the laptop. Since the computer is unable to sample at a high enough frequency, the spider takes the initial readings and stores it for later retrieval. The sampling frequency is 3200Hz. The recorded data was then compared to the performance estimation of the design program, as well as the FEA at similar conditions (refer: section 5 and 7).

Figure 28 Accelerometer mounted on model cage.

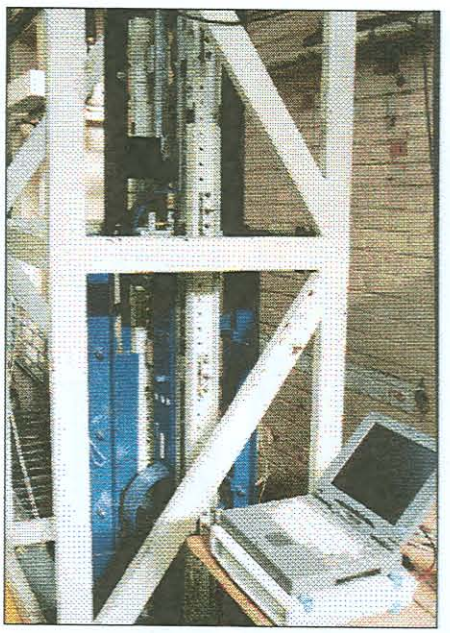

Figure 29 View of model and data capturing equipment.

The experimental procedure used to evaluate the performance of the arresting systems is as follows. The cage was hoisted to a set height above the installed arrestors, determined by the velocity that was to be achieved in the experiment, and released to fall freely. The cage velocity was measured by placing trip switches, a set distance apart, in the cage path. The time taken to trigger the switches was recorded and thus the velocity was calculated.

It was noted that a certain amount of friction occurs in the model's rails, since free-fall on achieved an acceleration of $8m/s^2$. This is understandable and would be encountered in full-scale situations as well. This has been compensated for in the programming of the design program, and can be easily adjusted to suit various conditions, as explained in section 5.1.2.

The model cage was then decelerated by the deformation process of the strips bending and unbending around the rollers, while being dragged through the roller sets. The process was triggered when the cage passed the cable contact point, which connected the two deceleration systems mounted to either side of the shaft walls (refer:Figure 30, Figure 31).

Figure 30 Loaded strips before cage impact.

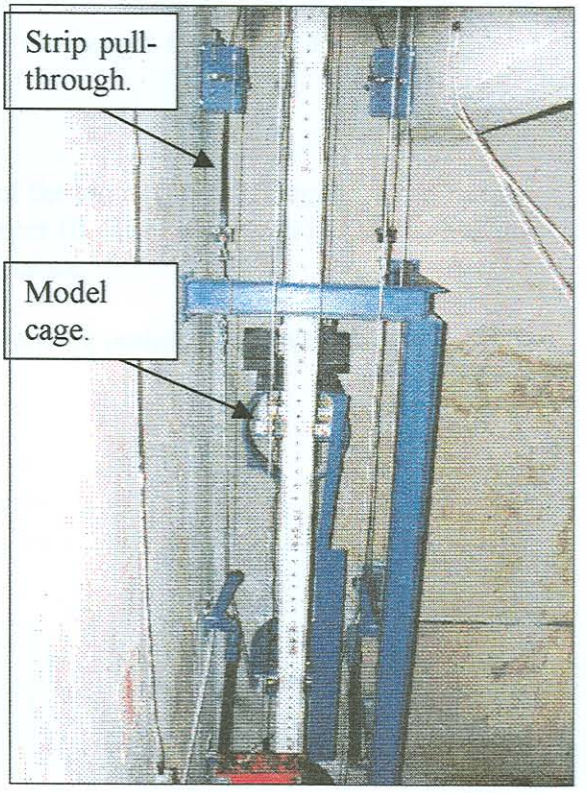

Figure 31 Pulled through strips, after impact.

6.2 Experimental model variables

Geometrical aspects of the model were identified as variables to be changed according to the arresting performance desired. Some of these variables were restricted in the experimental set-up and therefore only a few could be altered. The main reason for these restrictions was due to limited working space. The gap available to vary the roller size was limited, and would require a considerable amount of labour to change this, becoming financially and practically unviable. The space at the bottom of the model shaft, which was available to decelerate the cage, was also cramped in. As a result the achievable velocity for the cage was limited, since the braking distance available before reaching the bump-stops was only 1.5 meters.
The possible variables are the following.

- R = radius of the roller around which the strip bends.
- t = thickness of the strip.
- w = width of the strip. A taper has been introduced so there is a starting taper width and an end width.
- l = length of the taper.
- v = the velocity at which the process takes place was changed, which in turn influenced the strain rate of the material. This was varied by altering the height from which the model cage was dropped.
- M = the mass of the cage.

In the experimental procedure the thickness of the strip (t) was changed, as well as the width of the strip (w) and the length of the taper (l). The velocity (v) of the impacting cage was also varied by changing the drop distance.

The size of the rollers and the mass of the cage were maintained throughout.

6.3 Testing schedule

A testing schedule was set up to evaluate the program over a selection of conditions (refer: Figure 32).

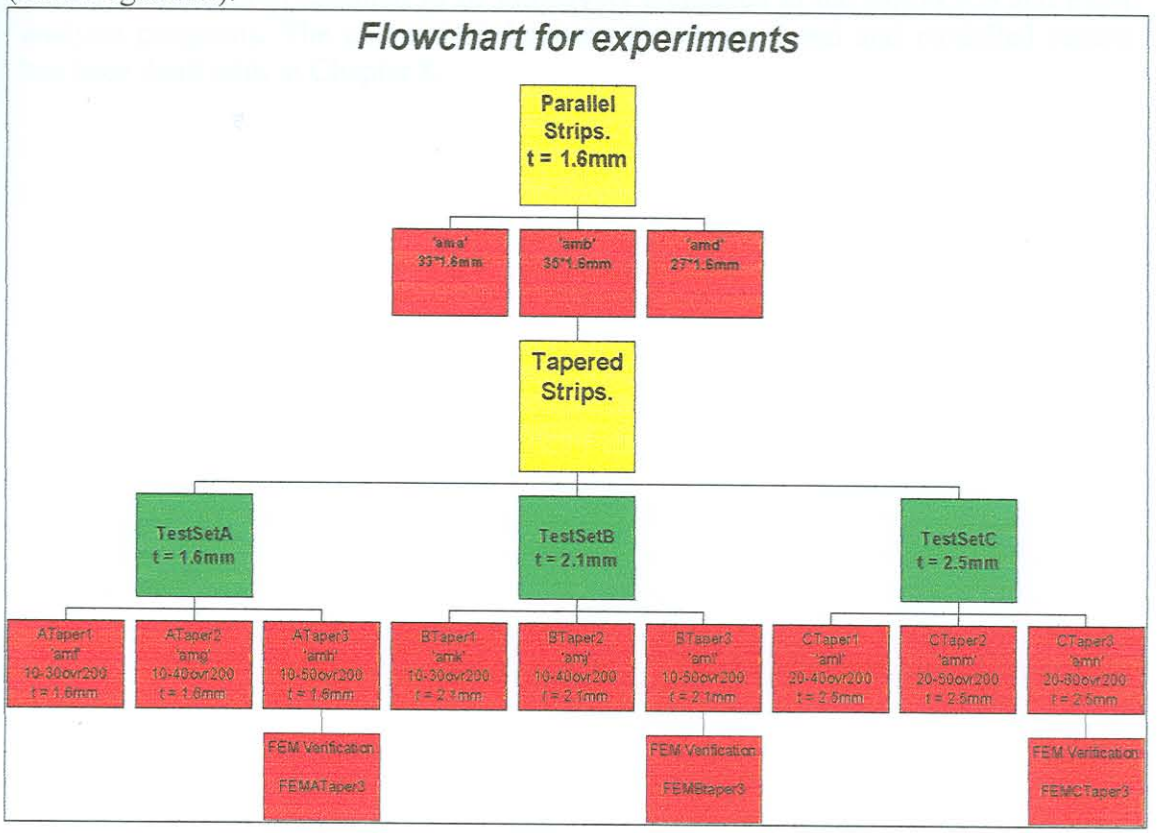

Figure 32 Testing schedule.

6.4 Experimental details

Figure 32 represents the entire history of testing for this project. The results of the parallel strip testing phase were considered as developmental and will not formally be dealt with in this manuscript. The results thereof are appended in Appendix C for interest sake and for the sake of completeness.

During the tapered strip phase of testing, TestSetA experiments were performed with a strip thickness of 1.6 millimetres (mm). The height from which the 130kg model cage was dropped was 1 meter (m). The taper profile increased as described in the flow diagram. 10-30ovr200 implies that the taper profile had a thin section of 10mm wide, increasing to 30mm over a distance of 200mm, and then remaining a uniform width for the remaining length (refer: Figure 17).

TestSetB experiments made use of a strip with thickness of 2.1mm and a drop height of 1.5 m. The taper profile variation for the scope of testing is described in Figure 32 as explained above.

TestSetC which was the final phase of testing, had a strip thickness of 2.5mm and drop height of 2.5 m. The taper profiles varied as described in Figure 32.

6.5 Experimental Conclusion

The experimental phase of the project determined the performance of the decelerating systems under various scaled down conditions. Considering the limitations, enough usable data has been captured to be effectively compared to the MATLAB and FEM analysis programs. The comparison between tested, predicted and modelled results has been dealt with in Chapter 8.

7. Dynamic Finite Element Simulation

7.1 Introduction

The finite element analysis (FEA) is a numerical method for solving problems of engineering and mathematical physics. Typical areas of application are structural analysis, heat transfer, fluid flow, mass transport and electromagnetic potential problems. For situations involving complicated geometry, loading and material properties, analytical equations are difficult to determine and solve. Hence, the numerical method of the FEA application is the only viable solution. The finite element formulation of the problem results in a system of simultaneous algebraic equations for solutions, rather than requiring solution of differential equations. These numerical methods yield approximate values of unknowns at discrete numbers of points in the continuum. The method of modelling a body by dividing it into an equivalent system of smaller bodies or units (finite elements) interconnected at points common to two or more elements (nodal points or nodes) and/or boundary lines and/or surfaces is called discretization. For an FEA the equations for each element are formed and combined to obtain the solution of the entire body, instead of solving the entire body in one step, as for the case with an analytical solution. Typically the solution of structural problems involves the determination of displacements for each node and the stresses within each element within the structure under the applied loads. With non-structural cases, the nodal unknowns would be temperatures or fluid fluxes, depending on the application.

The condition encountered in this FEA case is classified as structural impact. The reason for the FEA was to explore the geometrical limitations of the experimental scale model. The first limitation was the inability to change the roller diameter easily. In the experimental model this was physically difficult since there was limited space available. In the FEA it was a trivial exercise to change roller diameters. The geometrical factors which were readily varied in the experimental model were the strip thickness and the strip profile, the drop height and therefore the velocity. The second limitation was the under wind space available to decelerate the cage being limited, therefore restricting velocity range that could be experimentally simulated. Once again, the velocity of impact can easily be changed to suit the requirements in the FEA model.

During scale model testing, the data of accelerations experienced by the model conveyance was recorded (refer: section 6.). The finite element model (FEM) was then built (on computer) and dynamically excited to emulate the tested situations. For the purpose of this investigation, MSC Dytran was used for the FEA. The pre and post processing of the model was done in MSC Patran. The FEA results were compared to the tested readings and the comparison was of such accuracy that the FEA output was accepted as reliable and accurate. The maximum deviation was 25% and this is considered acceptable since the FEA was consistently non-conservative (refer: section 8.). A 25% error can at worst mean a 0.75g difference in a probable mine conveyance application where the limit is 2.5g. The envelope allowed for human deceleration is wide enough to compensate for the deviation (refer: Table 1). The accuracy of the FEA is considered adequate to form a comparative reference, against which to gauge the range of application of the MATLAB prediction program.

Having established the reliability of the FEM analysis output, the next step was to vary the roller radii, strip thickness and taper profile in the FEM for different situations and compare the data readings to the output predictions of the MATLAB design program. This simulation was used to further verify the accuracy of the design program.

An extreme situation involving a 40 tonne cage moving at 100 km/h was simulated and compared to the output of the MATLAB design program. The only difference between the two sets of results was the initial deceleration profiles (refer: Figure 33). In the figure showing the FEA velocity plot, a sharp decline in velocity at impact could be seen, where the design program output did not have the initial velocity dip. The reason for this is that the FEA takes the strip inertial impact into account and the design program does not. The mass of the strips capable of absorbing 15,5 mega joules of kinetic energy would be 900 kg each. (t = 20mm, R = 200mm, l = 18m, w = 380mm, material = 300W steel) In this case four strips would be required, so the combined mass of the strips, compared to the mass of the total system to be retarded, would be nearly 10%, which would have a significant inertial effect. In concept the following would occur: two masses collide, one of four tonnes (strips) and another of forty tonnes (cage). The initial dip in the velocity predicted by the FEM in Figure 33, was due to the inertial load caused by the forty tonne cage having to accelerate the four tonne mass. The forty tonne mass (cage) would have to accelerate the four tonne mass (strips), which is initially at rest, and since the strips are one tenth the mass of the cage, the deceleration effect on the cage is significant. After the initial deceleration, the combined mass would move on as a lumped mass body of forty-four tonnes. When the design program was fed the total mass, of the conveyance and the strips, (44 tonnes) the resulting velocity gradient of the FEM and the design program were the same. The only difference was the initial profile where the FEM took into account the mass ratio of the colliding masses and the design program did not, as depicted in Figure 33.

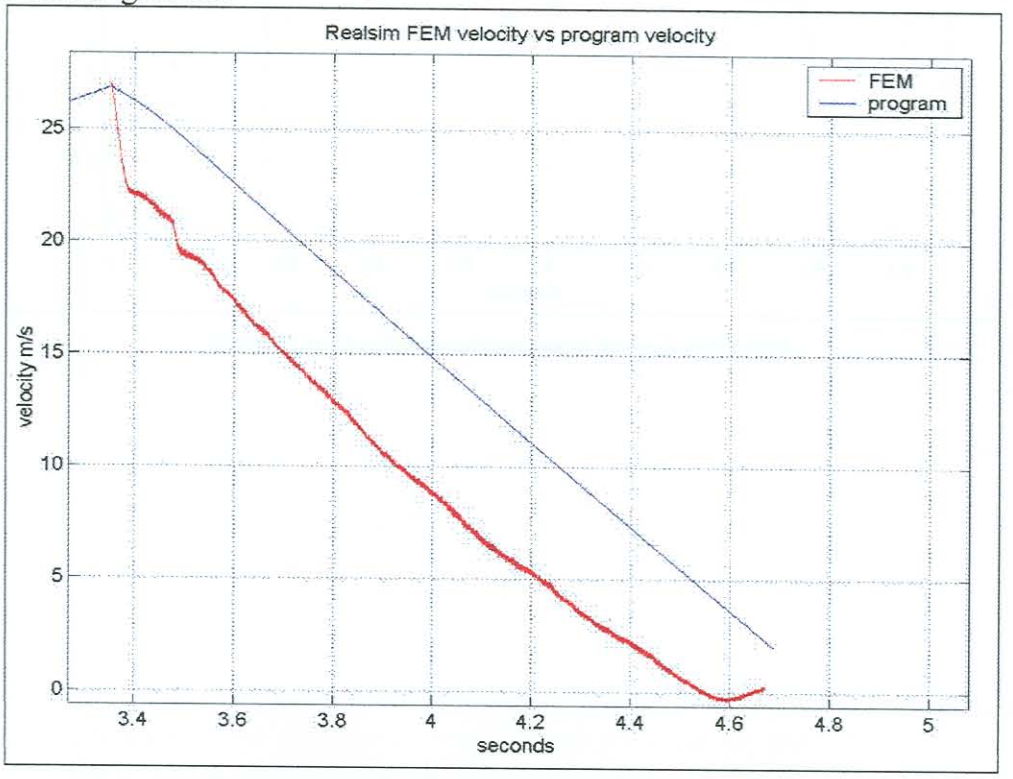

Figure 33 Velocity plot of program vs. its comparative FEM.

The initial velocity gradient drop of the FEM result as depicted in Figure 33, would result in a large impact deceleration effect experienced by the cage. This is confirmed in Figure 34 where the FEM acceleration plot has a high initial deceleration profile and then levels off to the same level as that of the design program, before coming to rest.

These conditions represented an extreme situation and it is unlikely that this would be encountered in a real life situation. This simulation was done purely to explore and identify the limitation of the design program and the possible scope of application.

It is still important to note that the time interval of exposure to the deceleration, had this event occurred, would have been in the order of three tenths of a second (refer: Figure 34). The FEM deceleration level peaked at four Gs for the impact and for that time interval would still have been safely within the survivable limits for head-ward (vertical) decelerations as discussed in section 2.1.2.

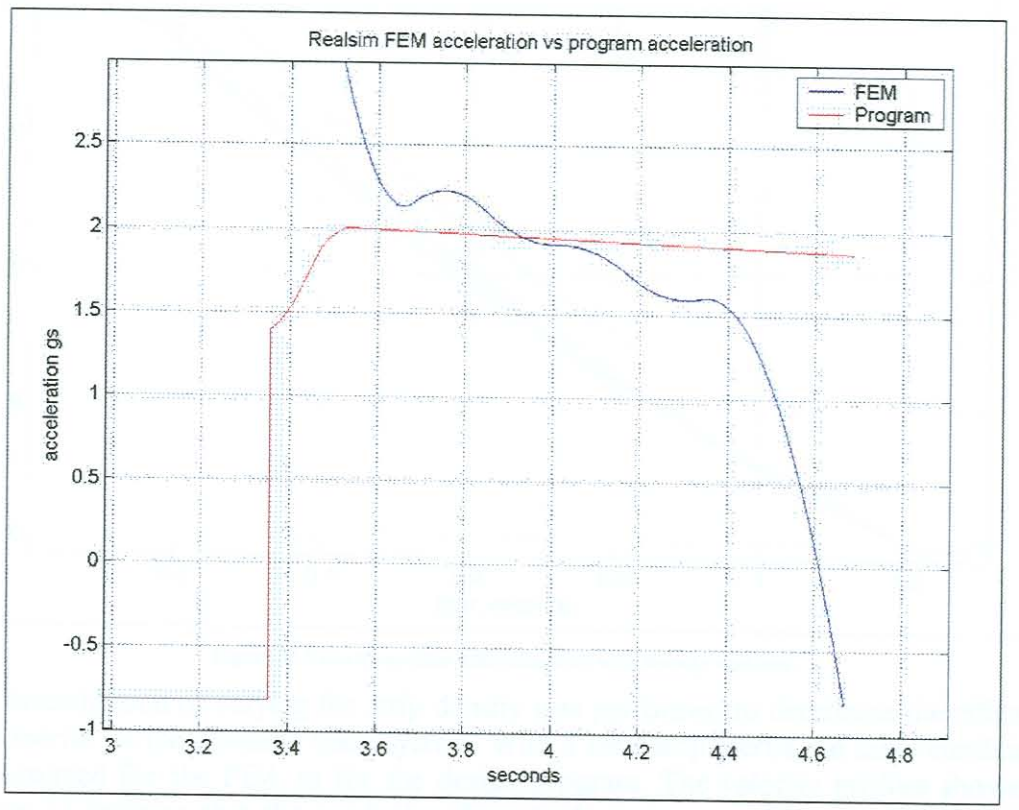

Figure 34 Acceleration plot of program vs. its comparative FEM.

A further investigation has been performed to determine the influence of the inertial effect on the performance of the braking systems. The capability of the FEA made it possible for the density of the strip material to be modified. The full-scale extreme condition, (as previously described) was simulated once more, but this time with strip element densities equal to 0% (1kg/m^3), 25% (1850kg/m^3) and 60% (6000kg/m^3). The resulting velocity and acceleration plots have been superimposed onto the previous 100% strip density condition and the differences were evaluated (refer: Figure 35, Figure 36).

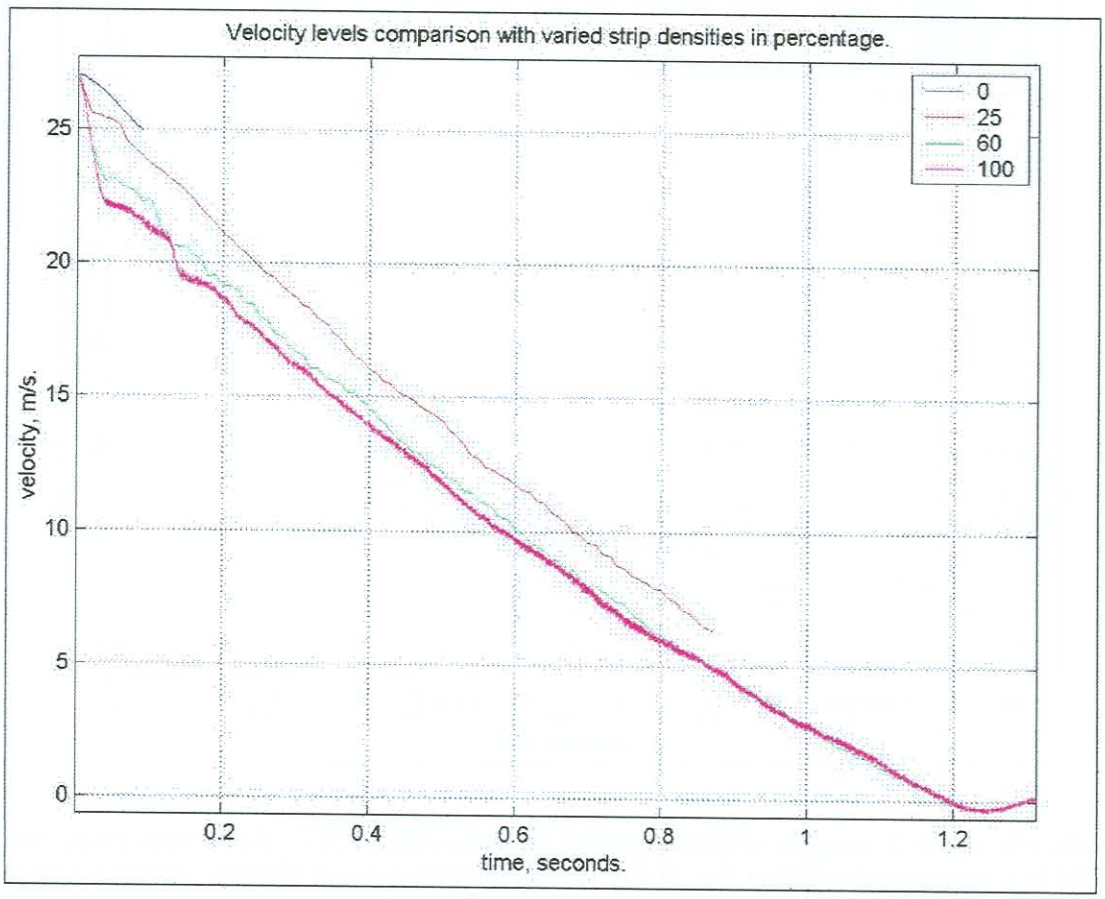

Figure 35 Velocity profiles difference with strip density variance.

The investigation of varying the strip density was performed to determine the effect of strip inertia on the colliding mass system. With a zero strip inertia the same conditions are assumed for the FEA as for the design program. The velocity profiles shown in Figure 33 indicate that the prediction from both sources are the same for the same conditions.

The selection of a low density for the 0% strip material density simulation, caused an extremely long computer running time of 110 hours for the data captured, covering only one tenth of the full event. For this reason the analysis was stopped prematurely revealing the short 0% curve in Figure 35. This still provided an indication of the gradient to be expected during deceleration and the effect of initial impact on the system.

A note can be made of the gradient change between the 0% and 25% curves, relative to the 100% curve. The gradient of the 0% and 25% curves are marginally steeper than the 100% density curve.

The acceleration curves in Figure 36 accentuated some important points. The first of these was the inertial deceleration effect. In Figure 36 curves FEM100 and FEM60 showed virtually the same initial deceleration levels. FEM25 was then substantially lower and finally FEM0 had an obvious trend of not showing inertial effects at all.
The second point highlighted was that the deceleration levels of all the cases, once past the impact zone, were at the same level.

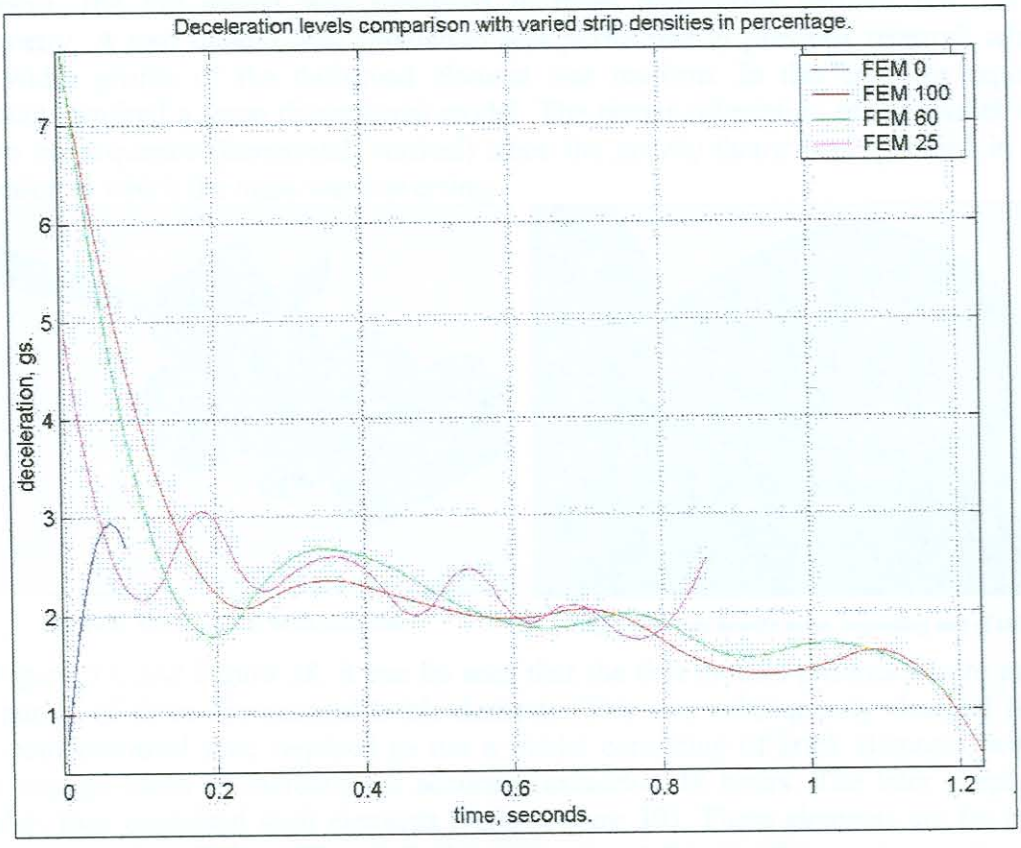

Figure 36 Acceleration profile comparison with strip density variance.

The compared results will be discussed in greater detail in chapter 8 where the three output sources, namely the experimental data, MATLAB prediction program and FEA are compared and evaluated in greater detail.

7.2 Model description

7.2.1 General Aspects

Due to the complex nature of the model, great manipulation and variation was required to produce a functional version. As a result of the dynamic nature of the scenario, the full model was simulated in three dimensions without the use of symmetry. A two dimensional simulation was performed in previous research where the width profile of the deformed element was uniform. In this case the tapered element required a three dimensional model. The planar orientation of the model was of no consequence (horizontal, vertical) since the gravity factor was specified in the direction in which the mass was traversing.

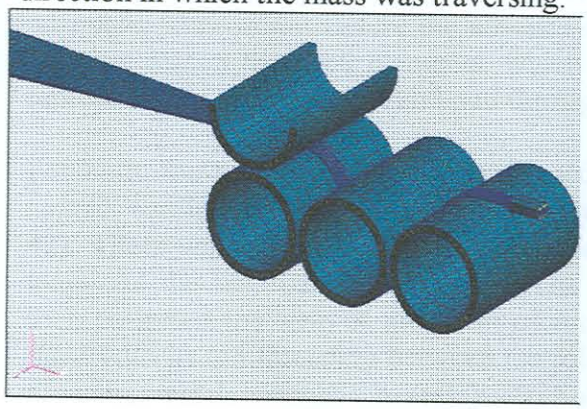

Figure 37 First model in brick elements.

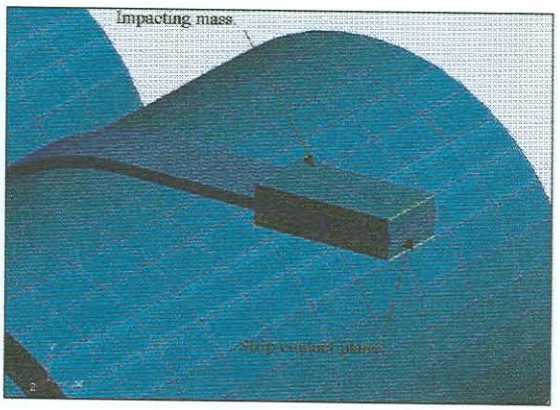

Figure 38 High density mass, impacting end of strip.

In Figure 37, and Figure 38, it can be seen that the first models produced were made up purely of three dimensional brick elements. This was subsequently changed since the computational time required to run a model consisting of brick elements, with a fine enough mesh to increase the accuracy exceeded 48 hours. The later simplified models thus contained shell elements (refer: Figure 39). These elements are far more computationally efficient. The shell elements were defined with a centre surface for every component. The surface was then meshed or divided into elements and given a thickness for each section as required to resemble the model to be simulated. It was possible to use shell elements since the material used was thin sheet metal. In the FEA model, only the relevant sections of the rollers were modelled. The non-participating sections of the rollers were omitted to improve the model's efficiency (refer: Figure 39).

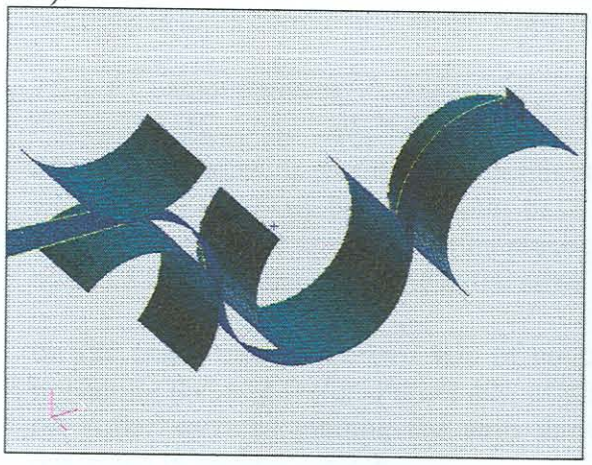

Figure 39 Shell element model.

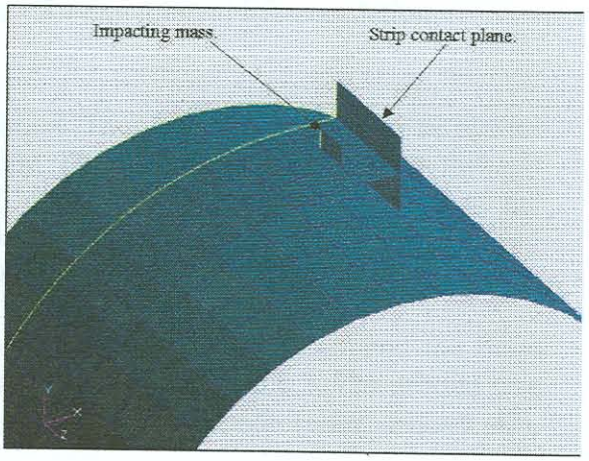

Figure 40 Shell mass surface and strip impact plane.

In this application the material deformation was not expected to be great, in terms of strain, since the bending of the strip took place around large curvatures. Although the component displacements were considerable, the strains are reasonably small. For the purpose of this study the points of interest were the deformation regions of the strip as it threaded between the rollers. The shell elements were capable of adequately predicting these events.

The strip was designed with a static safety factor of six, which is required by the Occupational Health and Safety Act for all lifting equipment with ropes or cables [21]. In this case the element can be regarded as a structural member and would thus only require a safety factor based upon good engineering judgement. A decision was made that for this application a factor of six based upon material yield limit was adequate. This would ensure the absence of necking in the thin section of the strip. For this reason the shell elements, which were selected, would deliver an accurate representation of the impact and pull through event.

For both, the brick and shell element models, the modus operandi was the same: a contact surface was defined between the roller sets and the strip itself (refer: Figure 42). There was also a contact surface created at the front of the strip, between the mass and the strip (refer: Figure 40). The mass was given an initial velocity, which then collected the strip at the point of impact. The strip was dragged along by the mass with its tail threading between the rollers, while applying a deceleration force to the mass, which brought it to rest (refer: Figure 39).

7.2.2 Constraints

In a FEA, many bodies are created, meshed and given material properties. When this process is completed the bodies must be combined into an assembly resembling the true scenario accurately. This is achieved by means of constraints.

Constraints are the definitions that are given to a model in order to closely describe the simulated scenario. These definitions can be applied in many ways, for example restricting motion, rotation or force applications. They represent mountings, initial velocities or contact surfaces. Many more situations could be applied, tailored to represent each unique real situation as accurately as possible.

Knowing how this particular system was to be used in practice enabled the choice of constraints to be confidently made, while not affecting the real life correlation.

7.2.2.1 Contact surfaces

Contact surfaces are inter-body, interface limits. These limits are defined as master and slave partners as was the case in this study. They indicate the boundaries through which other involved bodies cannot pass. This prohibits the interpenetration of the participating bodies and ensures the practical law of space, which cannot be occupied by more than one mass particle at the same instant.

In this study there were two sets of contact surfaces. The one simulated the mass impacting the strip (refer: Figure 40), as discussed in section 7.2.2.3. The second was the roller surfaces guiding the strip through the bending path (refer: Figure 42), described in section 7.2.2.2.

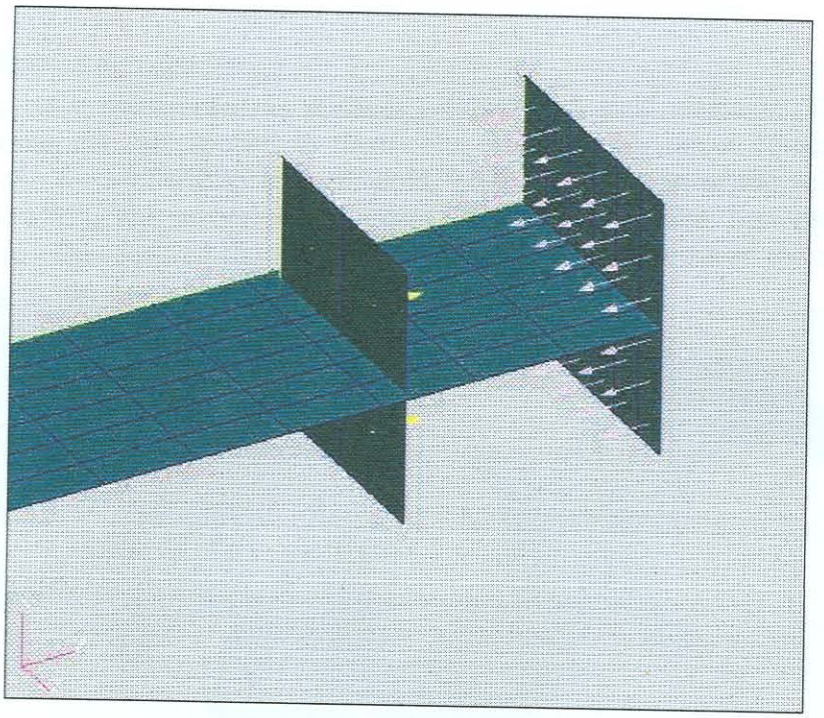

Figure 41 Mass and strip contact pair, master and slave.

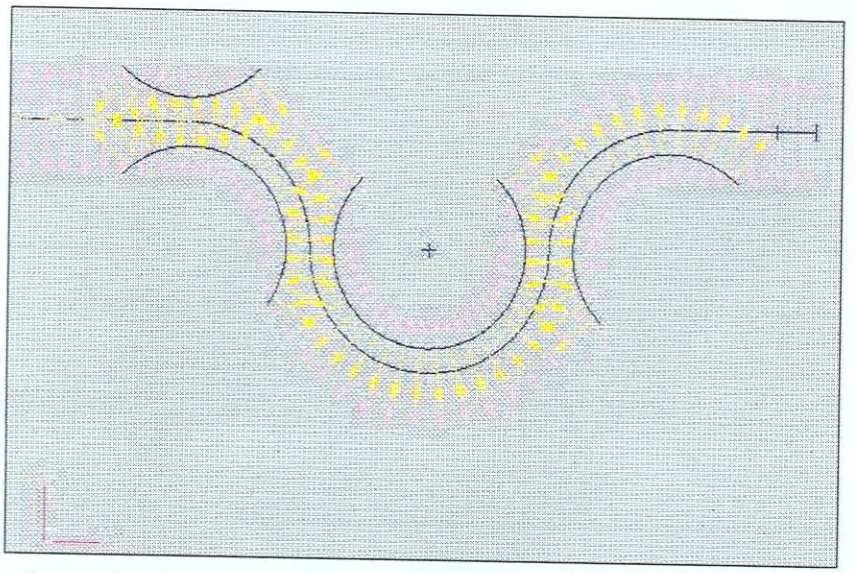

Figure 42 Strip and rollers contact pair, master and slave (Direction of contact support).

Figure 41 represents the contact mode definition of the mass surface. The yellow and purple arrows indicate the direction in which the surface was expecting contact from its master or slave partner.

In Figure 42, the pink arrows point in both directions, thus the strip expected contact from the rollers from both sides. The rollers were only defined in one direction, supporting and guiding the strip. The one direction of contact for the rollers was indicated by means of the yellow arrows. It was defined from the roller towards the strip, for each roller. The correct definition of the expected directions of interaction from neighbouring bodies in the model, drastically decreased the computational time of the analysis.

7.2.2.2 Rollers

The rollers were represented as surfaces meshed with shell elements. These rollers had two constraint sets applied to them. The first was the mount constraint that is applied in the form of a displacement hold, preventing motion of the roller surfaces (refer: Figure 43). The second was the contact surface constraint, between the rollers and the strip. This ensured the strip to travel along the path between the rollers while conforming to the arcs (refer: Figure 44).

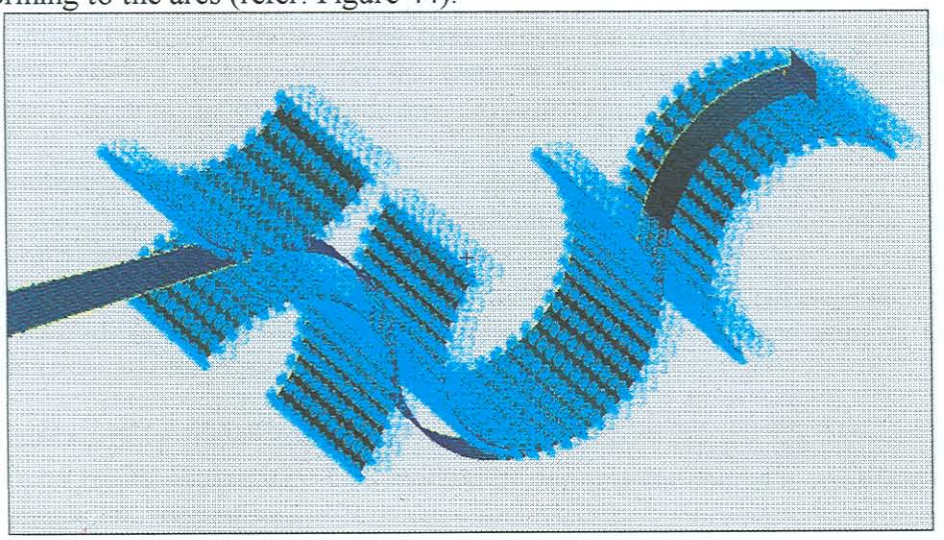

Figure 43 Displacement constraint definition of rollers

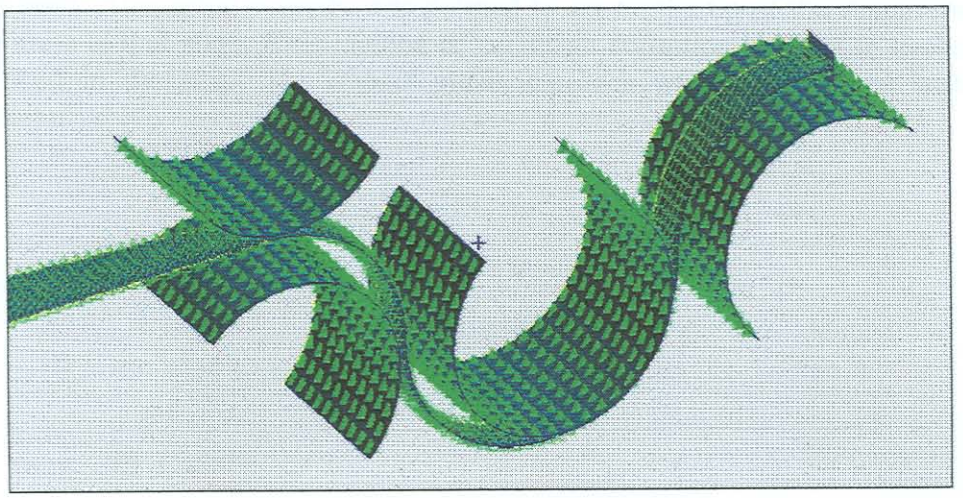

Figure 44 Contact constraint definition of rollers

The light blue points on the rollers in Figure 43 indicate the applied constraint at the nodes. In this analysis they prohibited displacement in the X,Y and Z directions. The rollers were therefore portrayed as stationary surfaces.

The contact between the strip and rollers was also discussed in section 7.2.2.1. In Figure 44 the solid triangles indicate the master surface and the empty triangles show the slave surface. The friction force between surfaces was simulated as zero since the experimental model rollers were mounted on bearings. For this analysis it was assumed that the friction force contribution from the rollers was negligible.

7.2.2.3 The impacting mass

The impacting mass was also represented by a surface and defined as shell elements. Gravitational acceleration was simulated as a constant acceleration in the direction of motion.

It had three constraints applied to it:

An initial velocity, which varies from model to model, depending on the impact severity needed. It allowed for the mass to be moving at the defined speed at the moment the analysis was started (refer: Figure 45).

Movement was restricted to only the X direction, since the situation of application is such that the strip would be drawn through the rollers by means of a cable (refer: Figure 3) towards a fixed point, the pulley. With this in mind, the assumption of planar motion was representative. In Figure 46 the blue dots represent the nodal Y and Z direction, displacement constraint. The same constraint was applied to both the strips ends, and the mass centre.

Contact surfaces (refer: section 7.2.2.1) were defined between the end of the strip and the mass (refer: Figure 47). This method of defining the model's conditions ensured a representative simulation.

An earlier attempt of simulating the scenario was to model the mass and the strip as one body. The initial velocity was defined to act on the tip of the strip, representing the mass at that stage. This method of condition definition resulted in necking being induced in the strip. The impact plane approach was then adopted with greater success.

Referring to Figure 45, the mass plane and the strip seem to be merged. This is only a visual impression since they were modelled as separate entities. In the FEM the mass and the strip only interacted with each other once the impact planes met (refer: Figure 41). Before that occurred they had no effect on each other, even though they seem to be merged. Figure 45 shows the initial velocity definition applied to the mass. Figure 46 shows the definition of X-axis motion of the mass and the end of the strip. In Figure 47 the solid triangles represent the master surface and the empty triangles define the slave surface, between the mass and the end of the strip. Contact surfaces are defined as master and slave pairs, with no preference to which ones remain stationary or move.

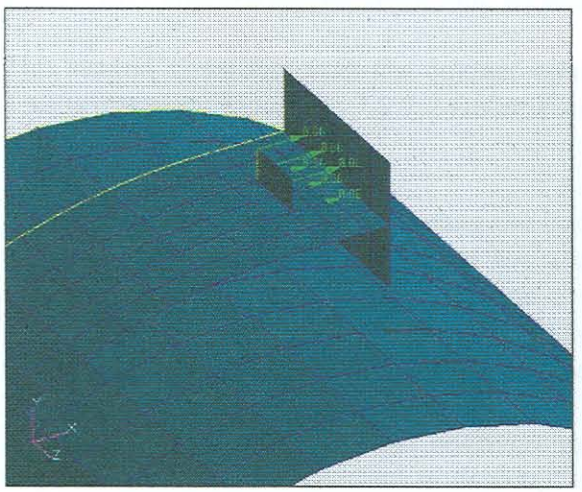

Figure 45 Mass initial velocity definition

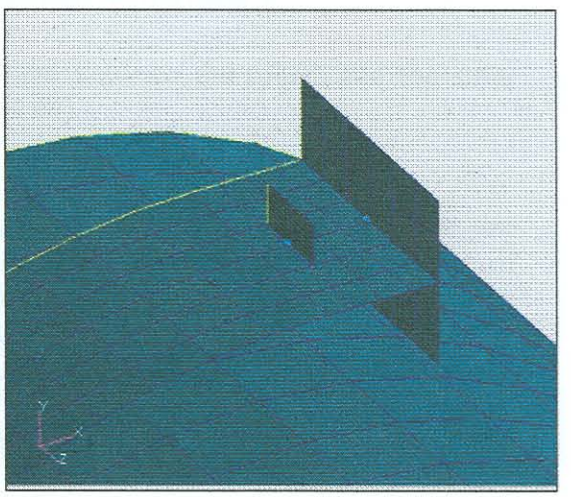

Figure 46 Mass and strip displacement guide

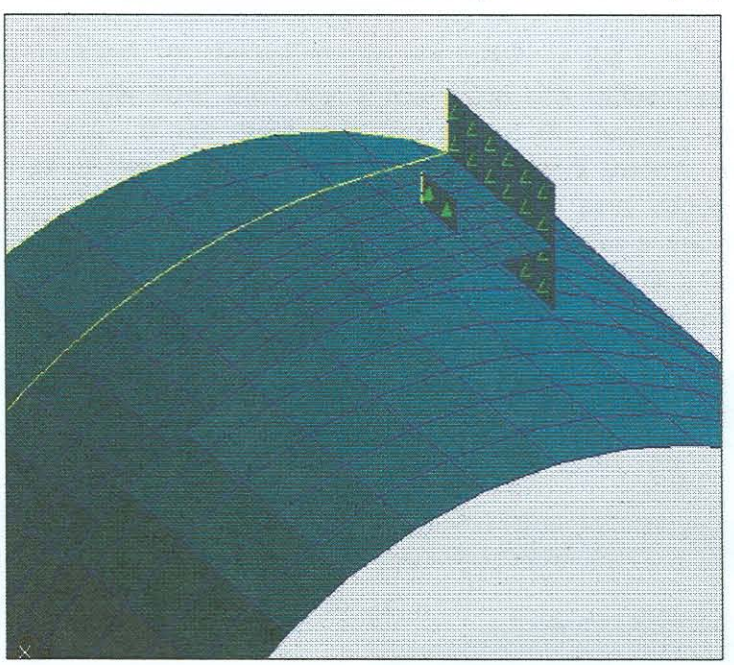

Figure 47 Mass and strip master and slave contact pair

7.2.2.4 The strip

For this analysis the strip was represented as a mid-surface and meshed with shell elements. There were two constraints applied to the strip.

The first constraint was a guide application. The constraint was applied by means of confining only one node on the front of the strip in the Y and Z direction, thus allowing only for travel in the X-axis. This was done to eliminate unnecessary degrees of freedom, which often occur in dynamic simulations. When there are too many degrees of freedom allowed, the models tend to diverge from real motion. (refer: Figure 46) (This is a similar constraint, as was applied on the mass.)

The second constraint was the contact constraint between the rollers and the strip. This is discussed in section 7.2.2.2 (refer: Figure 44).

7.2.3 Meshing

Meshing is the term used for dividing the body into blocks or finite elements. The size of the finite elements, greatly affect the accuracy of the FEA prediction. A rule of thumb is that the user specifies as fine a mesh as practically possible (processing power limitations influence this) in the expected high stress or critical areas in the geometry, to ensure a creditable degree of accuracy.

In this case the geometry was relatively simple and there was only one area that required some mesh refinement as depicted in Figure 48. This area was in the neck of the strip where the taper thins to its minimum width.

It was found that the mesh on the rollers did not influence the results significantly, however the mesh on the strip did play a roll since this influenced the bending performance of the strip. If the mesh was too coarse the bending arc would be simulated as a series of flat, disjointed surfaces and not as a smooth arc. The edge effect can be seen in Figure 49. The rollers (as indicated) have edges and are not smooth curves. The strip, shown between the rollers, clearly has a smoother surface. If the mesh on the strip were coarse, with similar edges as the rollers, a hooking rather than a sliding effect would have occurred. This would have obstructed the smooth pull-through of the strip.

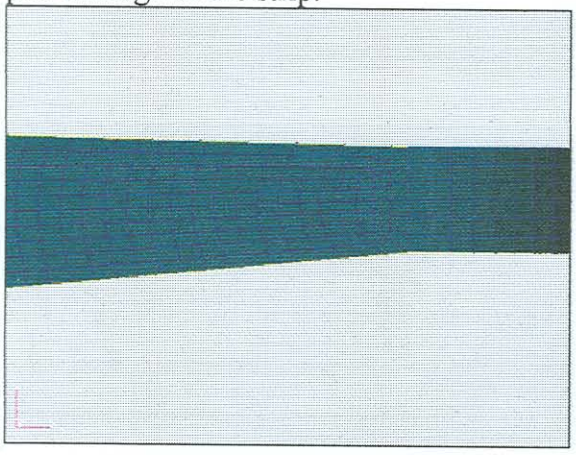

Figure 48 Strip mesh refinement.

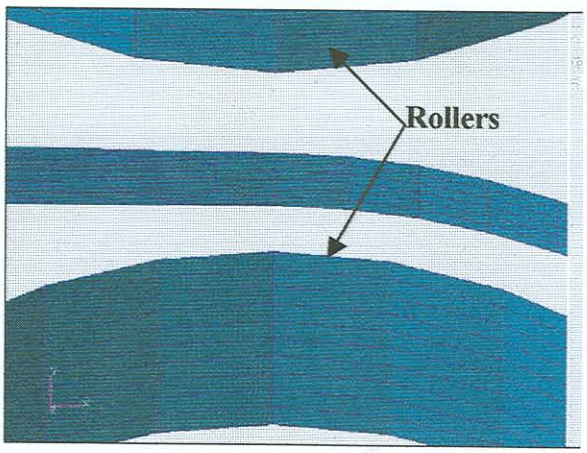

Figure 49 Strip and roller mesh difference.

7.2.4 Material properties

The material properties assigned to the various parts of the model are standard options in the FEM package. An advantage was that the Cowper Symonds (refer: section 4.3.1) material characteristics [8] were available as one of the constitutive models. This model was applied to the strip as discussed in section 7.2.2.4, since this was the component to be influenced by the high strain rate condition. The Cowper Symonds formulation has been used in the past to a great extent to accurately predict the performance of steel members under high strain rate conditions [7].

The rollers were given basic elastic plastic properties, as would be the case in standard steel under quasi-static circumstances. A density of 7800kg/m^3 as is the case for standard 300W mild steel.

For the impacting mass no great deformation was expected. A standard elastic plastic material property was thus assigned, with a variable density. The impact masses for the various simulations were heavy, but the impact areas were kept small, in order not to complicate the geometry. The mass was therefore simulated by means of an artificially high-density material to give the correct mass. Since no major part was played by the mass in terms of deformation, the consequences were considered to be minor.

7.3 The analysis

7.3.1 Analysis objectives

The objective of the finite element analysis phase in this study was to establish the accuracy of the code that was written. First of all a FEA benchmark was to be created, representing the experiments performed. The analysis plan was divided into three segments:

1. Simulation of experiments already done in the laboratory at the University of Pretoria to verify FEA accuracy, since the MATLAB code already showed close correlation to the experiments.
2. Simulate scenarios outside the practical experimental scope, in progressive stages of severity. The results are compared to the output of the MATLAB code for similar conditions.
3. Simulation of the real life scenario. The same scenario was fed into the MATLAB program and the results of both were compared to determine the degree of accuracy of the MATLAB code, when applied to the full-scale industrial conditions.

The stages of progression were followed in the above mentioned order, to establish where the MATLAB code output, and the FEM analysis output, diverge.

Verification of FEA relative to experiments performed.		
ATaper3	Btaper3	CTaper3
Taper = 10-50ovr200 t = 1.6mm R = 30mm Drop height = 1m	Taper = 10-50ovr200 t = 2.1mm R = 30mm Drop height = 1.5m	Taper = 30-50ovr200 t = 2.5mm R = 30mm Drop height = 2.5m

Exploring the experimental restrictions with FEA	
DeltaRoll1	Taper = 30-60over300 t = 6mm R = 80mm Velocity= 8m/s Mass = 500kg
DeltaRoll2	Taper = 40-100over500 t = 10mm R = 150mm Velocity= 12.5m/s Mass = 1000kg
DeltaRoll3	Taper = 100-250over1500 t = 20mm R = 300mm Velocity= 18m/s Mass = 5000kg

Full scale simulation. (4 roller sets, Mass = 40Tonnes, velocity = 100km/h)	
RealSim	Taper = 220-320over3000 t = 20mm R = 300mm Velocity= 27m/s Mass = 10000kg (per roller set)

Figure 50 FEM analysis Verification and Benchmarking Specifications.

7.3.2 FEA output

The output generated by the FEA was displacement of each element in the finite element model. From the displacement relative to time output, velocity was calculated. These results are closely compared to those produced by the MATLAB code and are discussed in detail in chapter 8. The FEA program used to perform the dynamic simulation also has the capability to deliver a visual display of what the model under went during the analysis. This function greatly enhanced the understanding of the process which took place during the deceleration event. A series of frames of one such play-back is shown in the following images, Figure 51 to Figure 54.

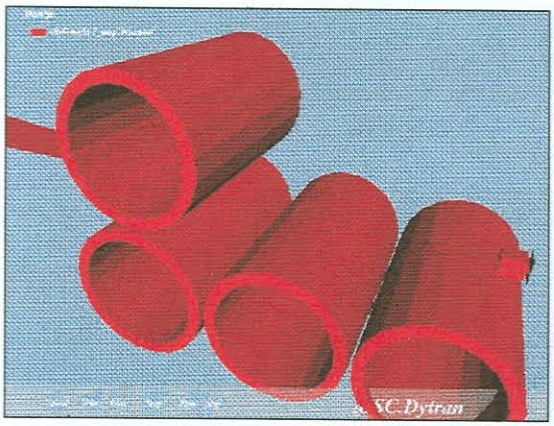

Figure 51 Threaded taper strip before impact.

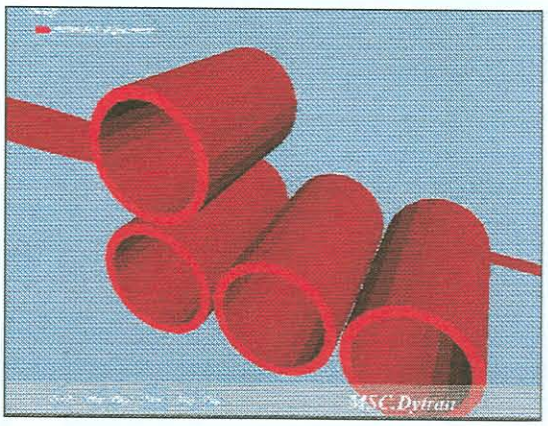

Figure 52 Threaded taper strip after impact.

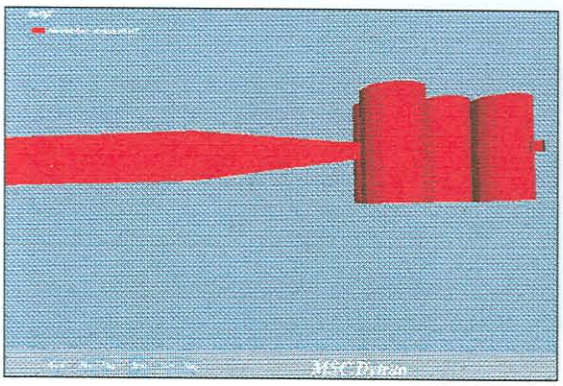

Figure 53 Top view of arrestor set, showing taper strip before impact.

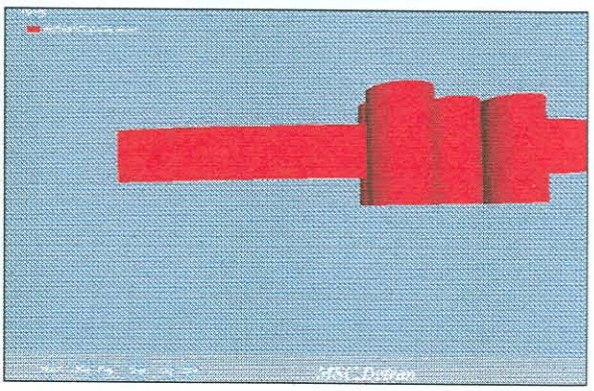

Figure 54 Top view of arrestor set, showing taper strip after impact.

Figure 51 illustrates the visual output prior to impact of the high-density mass, with the surface on the end of the strip. In section 7.2.2.3 the process of the mass colliding with strip and drawing it through the rollers is clearly explained. Figure 52 depicts the strip having progressed through the rollers for a certain distance. Figure 53 and Figure 54 show the top view of the same situations as the aforementioned, displaying the taper section of the strip moving through the roller assembly.

The following images are sequential images of an analysis playback, showing the progression of the strip being drawn between the rollers by the travelling mass, until finally coming to rest. The fact that gravity in the analysis is set to operate in the direction that the mass is moving should be kept in mind with regard to this example. The geometrical scale of the mass in the analysis is also not representative of the true mass used. This aspect is discussed in section 7.2.4.

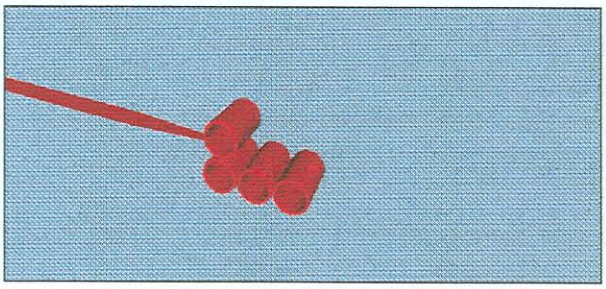

Figure 55 Arrestor set before impact.

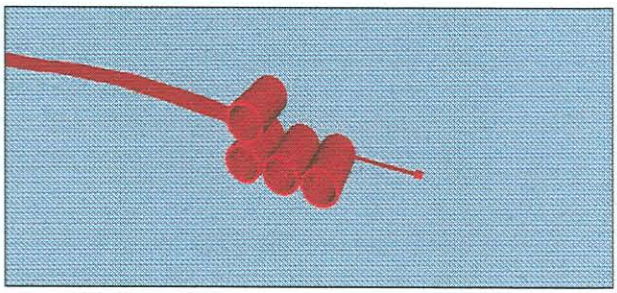

Figure 56 Strip being drawn through after impact

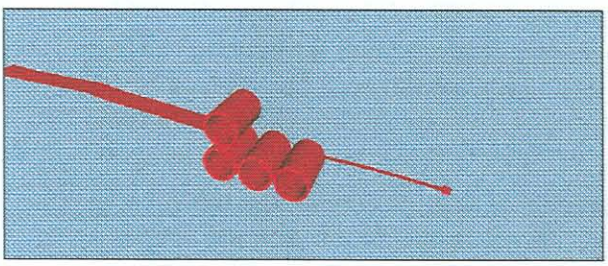

Figure 57 Strip taper section passing through rollers.

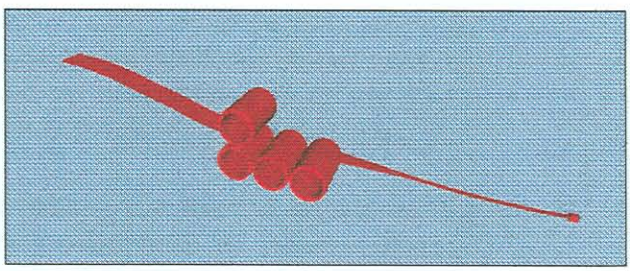

Figure 58 Strip parallel section between rollers.

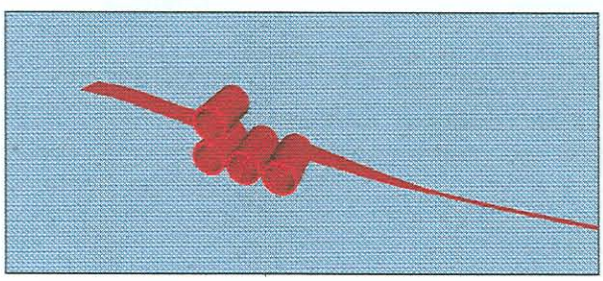

Figure 59 Strip at rest after deceleration complete.

7.4 Conclusion

The finite element analysis program DYTRAN, delivered sound information confirming the generated results delivered by the MATLAB code and the recorded experimental data. The details of these results have been discussed at length in the next chapter.